



Forest Fire Characterization Using Landsat-8 Satellite Data in Dalma Wildlife Sanctuary

Satendra Kumar Chaudhary¹ · Arvind Chandra Pandey¹ · Bikash Ranjan Parida¹

Received: 18 April 2022 / Revised: 9 September 2022 / Accepted: 14 September 2022 / Published online: 7 October 2022
© The Author(s), under exclusive licence to Springer Nature Switzerland AG 2022

Abstract

A forest fire has caused a loss of biodiversity and forest heterogeneity and resulted in forest degradation and fragmentation. Remote sensing techniques have been widely used for locating and delineating forest fires. The present study has employed Landsat-8 satellite data during 2014–2020 for spatiotemporal analysis of forest fire in Dalma Wildlife Sanctuary (DWS). Normalized burn ratio (NBR) has been used to delineate forest fire-affected locations along with visual interpretation techniques. The results showed that an extensive area was burnt and deforested due to forest fire in DWS during 2014–2020. The burned areas due to forest fires within the notified forest boundary in DWS were 12.11 km², 25.5 km², 22.45 km², 9.11 km², 24.44 km², 10.09 km², and 1 km² during 2014, 2015, 2016, 2017, 2018, 2019, and 2020, respectively, whereas burned areas outside notified boundary were 2.24 km², 4.15 km², 1.48 km², 3.29 km², 3.31 km², 1.9 km², and 0.1 km². According to visual image interpretation, the highest burned area was found in 2015 (25.5 km²), whilst the least affected was found in 2020 (1 km²), and fires were mainly seen in the degraded forests and open forest regions. The present study revealed that forest fire is more dominant in Asanbani, Pardih, Bhelaipahari, Gobargushi, Bamri, Andharjhor, Somadih, Koira, Tetla, Bochkamkocha, Sah, Rbera, and Jamdih locations/beats in DWS. Thereby, these forest beats need attention from forest managers to control fire-mediated forest degradation for the conservation and restoration of forests in DWS.

Keywords Forest fire · Remote sensing · NBR · Forest degradation

1 Introduction

Forest fire is a natural and human-induced risk and poses a principal threat to ecologically fragile regions across the globe. Most of the forest fire activities are primarily seen in tropical, sub-tropical forest ecosystems and savannas which evokes a threat to the sustainability of forests along with climate change [1, 2]. Over the recent decades (2000–2020), global warming and weather patterns have supported increasing forest fire frequency that suggests forest fire could have adverse impacts on the forest ecosystem at regional to global scales [3–5]. A widespread forest fire can lead to a decline in forest heterogeneity and biodiversity [6, 7], which further results in forest degradation and fragmentation and also prevents vegetation recovery [8]. Nearly 50% of forest

covers in India are prone to forest fires [9]. Various factors, such as climate, weather, physiographical structures, forest types, and anthropogenic activities, are the major features that influence forest fires in India [10, 11]. However, nearly 90% of forest fire in India was due to anthropogenic activity (e.g., collections of forest products, tourism, and other factors that cause fire frequently [10]. Human movements in the forest premises also increase the occurrence of forest fires [12]. Therefore, understanding the factors influencing forest fire can help to observe fire risk [13]. Numerous studies reported that forest fires generally occurred from February to May (pre-monsoon) in India [11, 14]. The forest types that are prone to fires are evergreen broadleaf and needle-leaf forests, deciduous broadleaf, mixed forest, shrubland, savannas, and grassland [15, 16].

Remote sensing (RS) based on multi-temporal data and geospatial techniques has been extensively deployed for monitoring and characterizing forest health and forest fires [17, 18]. Especially in forest fire studies, thermal RS has significantly contributed to detecting active fire, burnt area, fire risk, burn severity, and fire frequency [11, 19, 20]. Zhu

✉ Arvind Chandra Pandey
arvindchandrap@yahoo.com

¹ Department of Geoinformatics, School of Natural Resource Management, Central University of Jharkhand, Ranchi 835222, India

et al. (2006)[18] demarcated the extent of fire-affected areas based on the band combination of near-infrared (NIR) and short-wave infrared (SWIR) regions of the electromagnetic spectrum. Hence, RS has given wide opportunities for qualitative and quantitative analysis of forest fires at different spatial scales. It is also deployed effectively for monitoring and detecting forest fires [11]. In particular, Landsat satellite data have been employed for retrieving key information to map damaged areas accurately (both burned area and burn severity level) and quasi-immediately after forest fires [21–23].

Both space and airborne sensors have been utilized to map burnt areas, assess characteristics of active fires, and characterize post-fire ecological effects. Currently, several satellite-based sensors, such as IRS AWiFS/LISS, Landsat TM/ETM⁺, SPOT, ASTER, AVHRR, and MODIS, among others, provide synergistic datasets that have potential for forest fire detection and damage assessment. Landsat data were widely utilized for mapping smaller fire pixels which were further used for fulfilling the needs of local management [24–26]. Some of these studies have evaluated burnt severity based on Sentinel-2 Multispectral Instrument (MSI) data. Additionally, some studies [27, 28] demonstrated the suitability and even superiority of Sentinel-2 MSI data in natural resources applications. Several studies showed the changes in spectral properties of forest fire as compared to pre-fire conditions [29–32]. The assessment of forest fire burnt area is highly dependent on the acquisition date of satellite data. It is because of the timing of the occurrence of forest fire since the forest's spectral evidence or the quantity and character of the ash produced due to fire will be transformed by meteorological processes and regeneration of healthy vegetation [33]. Moderate Resolutions Imaging Spectro-Radiometer (MODIS) burned area products have been extensively used in detecting, monitoring, and characterization of forest fires [4, 34]. It provides information on different fire characteristics, such as location, the timing of active fires, a burned area, dry areas susceptible to wildfire outbreaks, and pyrogenic trace gas and aerosol emissions, among others. MODIS satellite sensor (Aqua/Terra) provides near-real-time fire alerts with 1 × 1 km spatial resolution. MODIS fire products have been evaluated in several independent studies [35–37], and the global MODIS fire algorithm was deployed for many specific regions across the globe [38–40].

Forest fire is a major problem in the state of Jharkhand in India because a forest in Jharkhand spreads over an area of 23,605 km², which constitutes about 29.61% of the total geographical area of Jharkhand [41]. About 82% of the area falls under protected forests, whereas 17.5% of the land falls under reserve forests. The main forest group of the state, as per Champion and Seth, is tropical dry deciduous forests, covering 93.25% of the total forest area of the state [42]. In 2010, a high frequency of forest fire was observed

in Jharkhand and extreme conditions, such as precipitation, temperature, relative humidity, and solar radiation, were found to be responsible for it [41]. In 2010, Jharkhand received 47% less precipitation, which was also declared drought-affected by the state government [41]. Keeping in view of a high incidence of forest fire in the protected forest in Jharkhand, the present study aimed to map burnt areas, detect active fires, and identify locations with recurrence of forest fire within different types of forest in Dalma Wildlife Sanctuary situated in Jharkhand. To accomplish this study, Landsat-8 satellite data was employed during the pre-monsoon season (March–May) over the span of 2014 to 2020.

2 Study Area

Dalma Wildlife Sanctuary (henceforth, DWS) is situated in the Chota Nagpur Plateau and extends into portions of the East Singhbhum, Saraikela, and Khushawa districts of Jharkhand state in India. Geographically, it is located between latitude 22°46'30" N and 22°57' N and longitude between 86°3'15" E and 86°26'30" E (Fig. 1). The total geographical area of the DWS as notified in the Ministry of Environment and Forest act (MoEF) 1972 is 398.58 km². It is further classified into 6 beats, 26 sub-beats, and 85 blocks. According to the Survey of India (SOI) topographical map notified forest boundaries (NFB) within DWS, which cover 205.8 km² area and other areas consider outside the NFB exist at 193.5 km² areas. The forest cover exhibits various types of vegetation, such as northern tropical dry deciduous forest (sub-group-5B) and more specifically, (sub-type 5B/C1c) dry peninsular Sal and northern dry mixed deciduous forest (type 5B/C2).

Dalma top is situated within the core area of the sanctuary with the highest elevation of 926 m above the mean sea level (AMSL), although the average elevation is 154–544 m AMSL. The climate of DWS is hot and humid, with an average summer temperature of 38 °C [8]. The temperature difference between the foothill and hill slopes is about 15–20 °C, which has formed an abundance of flora and fauna. The average annual rainfall is 1447 mm (mean of 1951–2000) [43]. Dimna Lake is situated within the DWS boundary. The major river passed through the DWS is the Subarnarekha and forms the southern boundary along with the Jamshedpur industrial town.

3 Materials and Methods

3.1 Satellite Data Used

Landsat-8 multi-temporal satellite data (2014–2020) were used to delineate forest fire locations. The data was

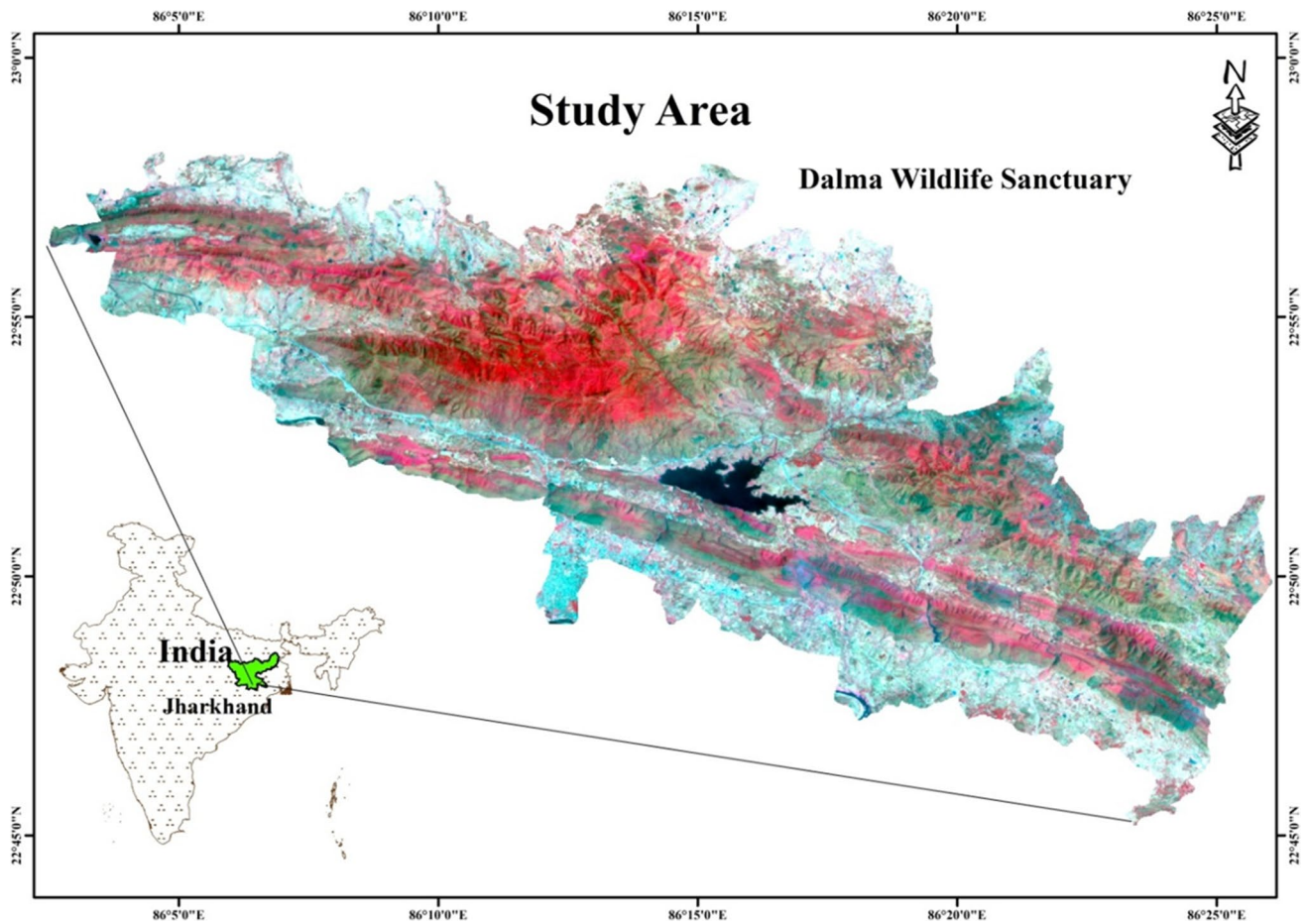


Fig. 1 Map showing the location of Dalma Wildlife Sanctuary. The false color composite (FCC) image depicts a thick forest along with the Dalma mountain range with Dimna Lake in the southernmost area

processed in GEE, and the details have been provided in Table 1. Forest fires are common in the dry deciduous forests of India during the summer months from March to May. Therefore, satellite data were acquired during the month of March to May to identify the forest fire and its impact on the forest ecosystem. In this study, satellite data were used to identify and delineate forest fire active areas inside the sanctuary based on pre and post forest fire satellite data analysis during 2014–2020. The data were acquired from the US Geological Survey (USGS).

The Landsat-8 has SWIR, NIR, and red bands, and among them, Operational Land Imager (OLI) sensor comprises a spatial resolution of 30 m. The SWIR, NIR, and red spectral bands of OLI sensors were found to be useful to delineate active forest fire locations since these bands are sensitive to a higher temperatures [44]. The SWIR, NIR, and red bands were assigned to the red, green, and blue colors, respectively, to highlight the active forest fire locations.

3.2 Field Data Collection

During field visits, it was observed that DWS dominates with dry deciduous forest types. Dry climate conditions in the summer season promote the rapid growth of forest fires in the dry deciduous forest types. Apart from high temperature-driven forest fires in the sanctuary, another cause of forest fire in the summer season was the collection of mahua flowers (*Madhuca longifolia*) by local people. For easy collection, people clean the area around mahua trees by burning the underneath dry leaves. During this process, sometimes people fail to extinguish the fire, and such fire becomes uncontrolled and causes forest fires in the area (as shown in Fig. 2).

3.3 Methods

3.3.1 Visual Interpretation for Locating Forest Fire

The visual interpretation was performed based on the color, patterns, shape, size, and texture of satellite imagery to

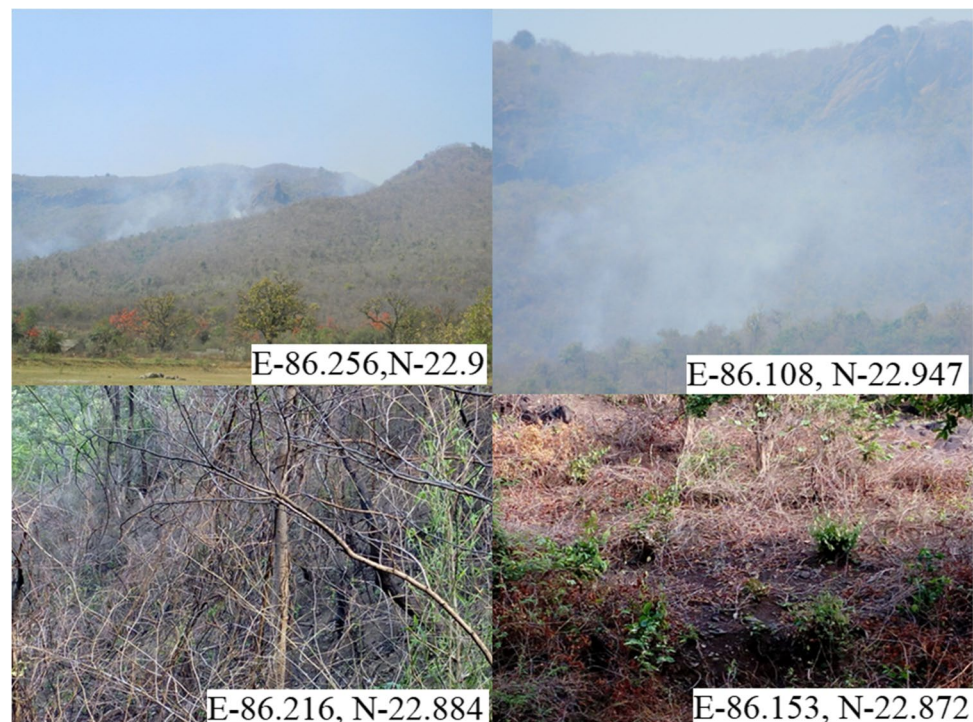
Table 1 Landsat-8 data used in the study and their acquisition dates

| Years | Pre-fire Acquisition dates | During fire Acquisition dates |
|-------|----------------------------|--|
| 2014 | 30 January 2014 | 4 March 2014 12 April 2014 29 April 2014 6 May 2014 |
| 2015 | 6 March 2015 | 22 March 2015 7 April 2015 9 May 2015 10 June 2015 |
| 2016 | 9 March 2016 | 24 March 2016 13 April 2016 25 April 2016 20 May 2016 |
| 2017 | 27 March 2017 | 28 April 2017 24 May 2017 |
| 2018 | 14 March 2018 | 15 April 2018 1 May 2018 21 May 2018 |
| 2019 | 17 March 2019 | 2 April 2019 27 April 2019 14 May 2019 |
| 2020 | 16 February 2020 | 28 March 2020 20 April 2020 15 May 2020 |

identify active forest fires and smoke. From the satellite images of different dates, forest fire and fire-induced smoke can be seen along with the fire spread areas of active forest fire zone by changing the false color composite (FCC) band combinations. For instance, aerosol and red bands (FCC of 4,1,1) combination indicates the smoke zone. The active fire was seen below the smoke zone in the band combination of SWIR-2, SWIR-1, and NIR (Bands: 7,6,5) at various locations in the sanctuary during the fire periods.

3.3.2 Forest Cover Classification

Forest cover classification was performed using Landsat-8 data based on normalized difference vegetation index (NDVI), which has been classified into five classes such as high dense, dense, open, degraded, and forest blank. The Survey of India (SOI) topographical sheet was used to delineate baseline information related to forest, non-forest, road network, and built-up. Incidents of forest fire generally take place in the Sal-dominated forest due to the dry leaf shading during the autumn season because the maximum area is covered with 5B/C1c dry peninsular Sal Forest in DWS. Therefore, to understand the fire locations with reference to the forest type, forest fire locations, pixels were further converted into vector format in ArcGIS software and then overlaid with the generated forest classification map to identify the relationship between forest fire and forest types affected by the fire. The schematic diagram of the methodology is shown in Fig. 3.

Fig. 2 Forest fire locations in Dalma Wildlife Sanctuary

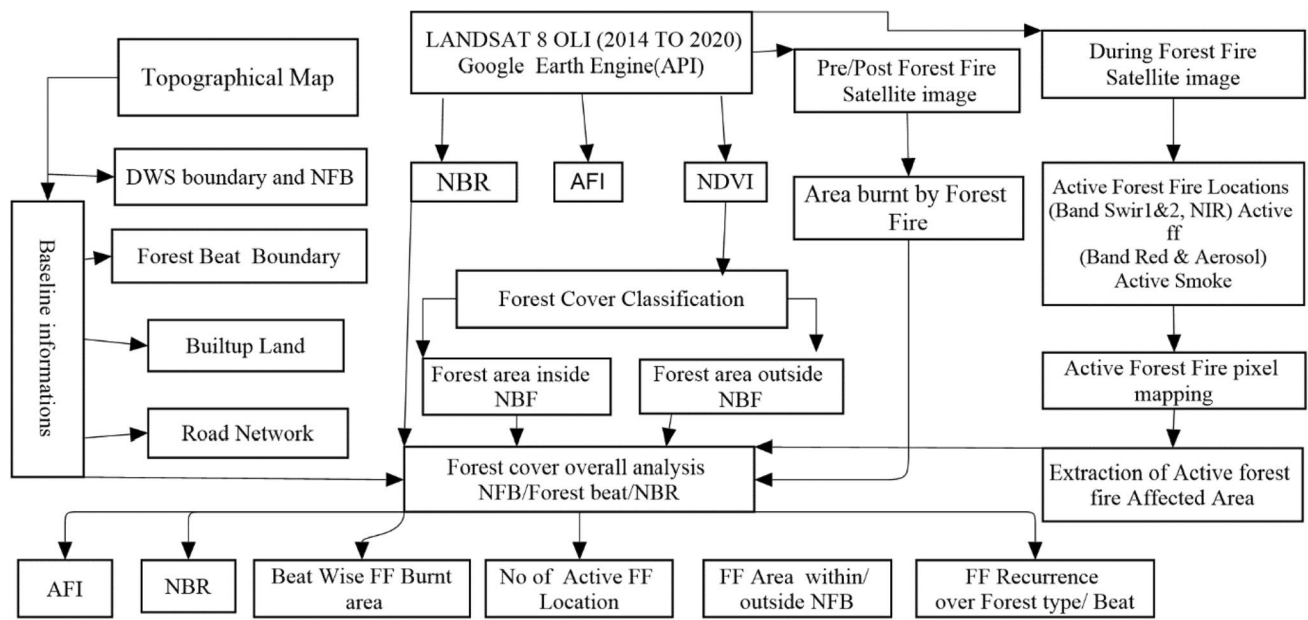


Fig. 3 Methodology adopted to study forest fires over the period 2014 to 2020

3.3.3 Indices for Locating Forest Fire

Normalized burn ration (NBR) is capable ($NBR = NIR - SWIR\ 2 / NIR + SWIR\ 2$) to generate a burn severity map and assessment of forest fire areas affected by a forest fire. NBR helps to identify for highlight burned areas. Forest fire intensity represents the energy that is released from organic matter during the combustion process [45]. After a forest fire, burned areas have low reflectance in the NIR and high reflectance in the SWIR band. The NBR is calculated for images before the fire (pre-fire NBR) and for images after the fire (post-fire NBR). The post-fire image is then subtracted from the pre-fire image to create the differenced NBR (dNBR) image. dNBR can be used for burn severity assessment, as areas with higher dNBR values indicate more severe damage, whereas areas with negative dNBR values might show increased vegetation productivity.

3.3.4 Active Fire Index (AFI)

The analysis of thermal and spectral bands is the fundamental building block of fire detection strategies. The Landsat-8 sensor's Band 7 (or SWIR2) has previously been used to detect fire radiation [46]. In this study, the active fire index (AFI) has been derived from Eq. (1).

$$AFI = \frac{B7}{B2} \quad (1)$$

where B7 and B2 stand for the SWIR2 and blue bands, respectively, of the Landsat-8 (OLI) image. The forest fire

has a high reflectance in SWIR2 and a relatively low reflectance in the blue spectral regions that highlight it from the background. The other characteristic is eliminating smoke from the forest fire in the satellite image. Smoke reflects strongly in the blue spectral region but has lower reflectance in the SWIR2 band [47]. This difference in spectral behavior causes the AFI value to be low in the smoke-contaminated pixels. Actual fire pixels at the cloud boundary can be hidden by improper cloud masking [48]. The AFI value is low in the cloud-contaminated pixels because the cloud has higher reflectance in the visible spectrum than in SWIR2 [49].

4 Results and Discussion

4.1 Land Use and Land Cover (LULC) of DWS

The land use and land cover (LULC) map indicated that the majority of areas of DWS are dominated by forests (Fig. 4 and Table 2). Forest fire incidents were also observed during 2014–2020 in the sanctuary both inside and outside the notified forest boundaries (Fig. 4). The total area affected by forest fires inside the notified forest boundaries comprised 11.46 km², 25.45 km², 19.64 km², 8.44 km², 24.44 km², 25.45 km², and 1.1 km² from 2014 to 2020, respectively. The total area covered by degraded forest (59.06 km²) and open forest (49.84 km²) inside the NFB comprised the total forest area within NFB. The area lying outside of the notified forest boundary constitutes a large population with agricultural land use.

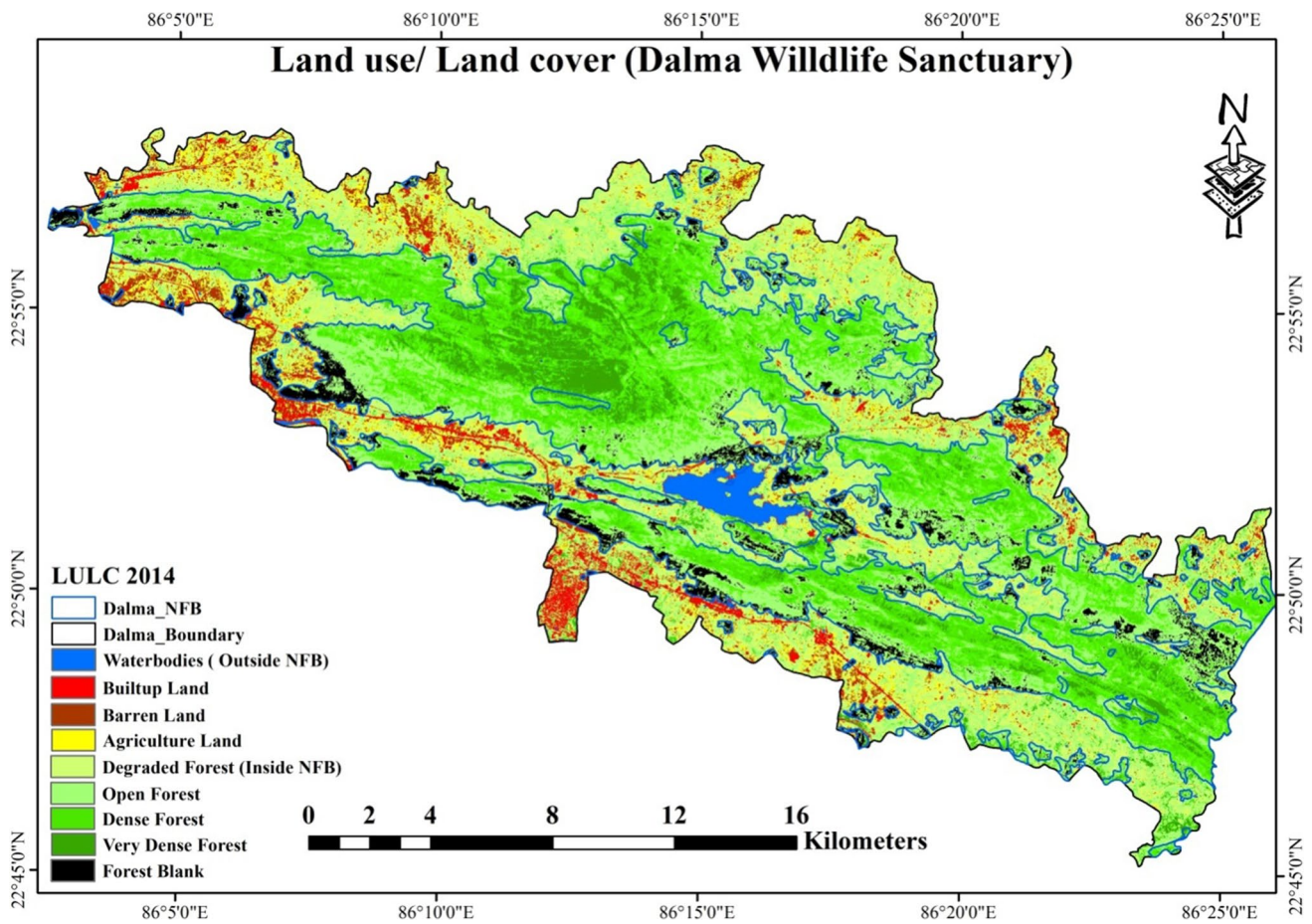


Fig. 4 Land use and land cover (LULC) map prepared from satellite image of 2014 in DWS inside notified forest boundary and outside notified forest boundary

Table 2 LULC classes with area statistics in km² categorized into notified forest boundary and outside notified forest boundary

| LULC | NFB | Outside NFB |
|-------------------|-------|-------------|
| Very dense forest | 18.50 | 4.85 |
| Dense forest | 46.31 | 42.17 |
| Open forest | 49.84 | 52.46 |
| Degraded forest | 59.06 | 47.57 |
| Forest blank | 19.9 | 0 |
| Water bodies | 0.33 | 5.106 |
| Built-up land | 0 | 11.92 |
| Barren land | 0 | 15.21 |
| Agriculture land | 0 | 26.64 |
| | 193.5 | 205.8 |

Forest fire burnt area outside NFB indicated that the major losses occurred in the degraded forest (47.57 km²) and open forest (52.46 km²) with forest fire-affected areas as 2.24 km² (2014), 4.15 km² (2015), and 1.48 km² (2016). In

contrast, inside highly dense forests and dense forest regions, as such, no forest fire incident happened both inside and outside NFB in DWS.

4.2 Active Forest Fire Detection in the FCC

Active forest fire flame and smoke during the forest fire over the period 2014 to 2020 were presented in Fig. 5 with reference to pre- and post-fire conditions in Fig. 6. The results revealed that during the forest fire, flames are noticed in the FCC image shown in Fig. 6, which were absent in the pre- and post-fire conditions. This observation was noticed across all years during the forest fire, according to visual interpretation. According to visual analysis, several fire locations and associated burned areas across 2014–2020 were given in Table 3. It was found that the maximum number of fire locations occurred in the year 2014 (40), followed by 2015 (29), 2018 (23), and 2016 (20). Whereas the minimum number of fire locations occurred in the year 2020 (02), followed by 2017 (05) and 2019 (08). Forest fire in DWS indicated that during the summer season (March to May), the forest cover

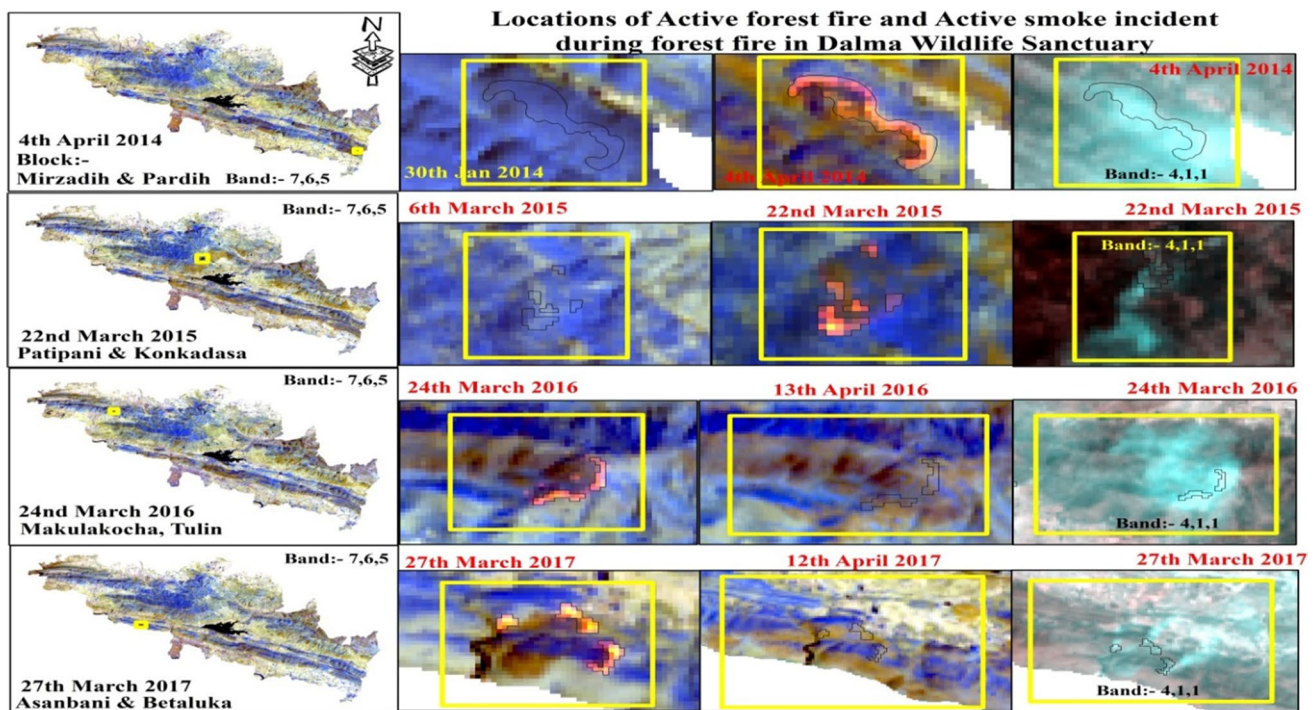


Fig. 5 Identifications of active forest fire flame and smoke during the forest fire in different locations of the sanctuary as observed on satellite data

remains under stress. Accordingly, the maximum burned area was estimated as 0.356 km^2 in the year 2016, while the least burned area of 0.010 km^2 was calculated in the year 2020, as shown in Table 3.

On the other hand, the addition of AFI highlights the number of forest fire pixels in Fig. 7. The visual interpretation with band combination of SWIR-2, SWIR-1, and NIR (7,6,5) of Landsat-8 OLI image showed that forest fire in DWS, as shown by AFI, is quite similar to Figs. 5 and 6. Hence, the results of forest fires in three different years are consistent in DWS irrespective of methods adopted.

4.3 Forest Fire Across the Year 2014 to 2020 Based on Visual Image Interpretation

In the year 2014, it was observed that 12.28 km^2 (3.08% of the total area of DWS) area burned due to forest fire, and 120 fire-affected locations were identified using temporal satellite data. The analysis indicated that all these forest beats of DWS, such as Chakulia (0.42 km^2), Mango (4.06 km^2), Dalma (1.69 km^2), Patmda (2.44 km^2), Nutandih (1.78 km^2), and Bhadodih (1.72 km^2), were influenced by forest fires. Most of the forest fires occurred in the southwestern part of the study area, including major locations at Gerua, Jhunjka, Jamdih, Tengadih, Koira, and Gobargushi. The maximum forest fire burnt area in Mango beat (4.06 km^2) where 21 forest fire patches were identified. Forest beat wise analysis

influenced by a forest fire during these years is shown in Table 4. The maximum number of forest fire locations identified in (29) places in Patmda beat. In the DWS, several roads and surrounding agricultural land induce incidence of forest fire, indicating fire occurred predominantly due to human intervention.

In 2015, it was observed that 29.61 km^2 of areas were affected by forest fire, with 263 fire-affected locations in the DWS. The analysis indicated that all the six forest beats of DWS were influenced by forest fire, whereas the forest beat was undercover with fire; Chakulia (0.52 km^2), Mango (10.40 km^2), Dalma (1.20 km^2), Patmda (6.19 km^2), Nutandih (3.12 km^2), and Bhadodih (4.11 km^2). The major locations of forest fire were at Mirzadih, Asanbani, Nutandih, Jhunjka, Jamdih, Ghorabandha, Appo, Betaluka, Gobargushi, Beldih, Andharjhor, Ramgarh, and Konkadasa, with the highest forest fire burnt area delineated in the Mango beat (10.40 km^2) within 61 forest fire locations (Table 4). The total geographical area of the Mango beat is 79.61 km^2 , of which about 8.27% was damaged due to forest fire. Fire locations in the Mango beat were sharing boundaries with nearby villages, indicating possible human interaction in forest fires.

In 2016, it was observed that 22.41 km^2 areas were affected by the forest fire, with 283 fire-affected locations in the Dalma wildlife sanctuary. The analysis revealed that all the six forest beats of DWS were influenced by forest fire:

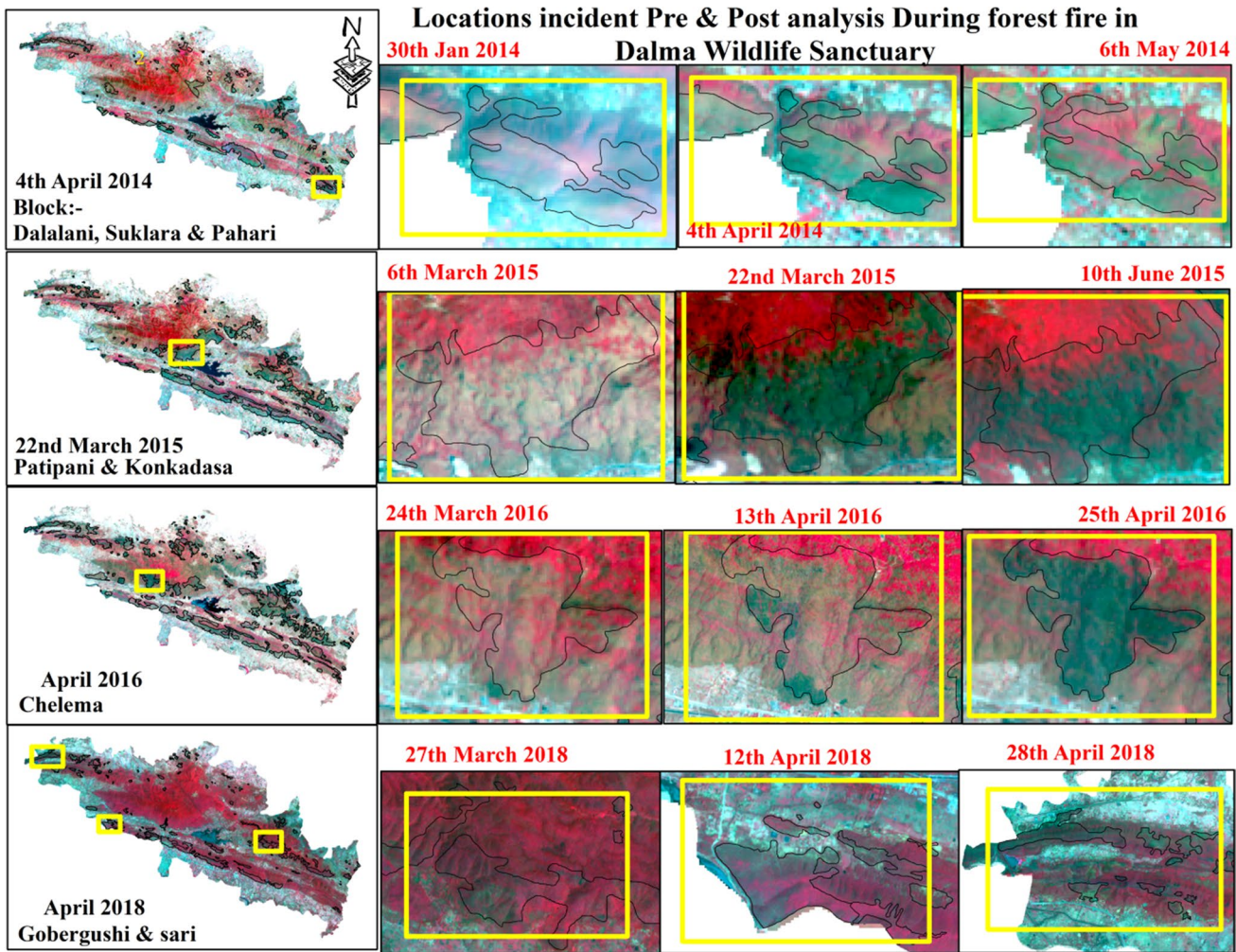


Fig. 6 Pre and post forest fire satellite data showing changes in the pattern of forest cover due to forest fire

Table 3 Number of fire locations and associated burned area across 2014–2020 as estimated based on visual interpretation

| Years | Number of fire locations | Burned area (km ²) |
|-------|--------------------------|--------------------------------|
| 2014 | 40 | 0.325 |
| 2015 | 29 | 0.232 |
| 2016 | 20 | 0.356 |
| 2017 | 05 | 0.066 |
| 2018 | 23 | 0.261 |
| 2019 | 08 | 0.18 |
| 2020 | 02 | 0.010 |

Chakulia (2.25 km²), Mango (5.95 km²), Dalma (5.67 km²), Patmda (3.01 km²), Nutandih (2.29 km²), and Bhadodih (3.28 km²) (Table 4). It was also observed that most of the forest fire-affected locations occupied the same locations where an earlier forest fire was recorded in the year 2015.

In 2017, it was observed that about 11.73 km² of areas were affected by the forest fire, with 160 fire-affected locations in the Dalma Wildlife Sanctuary. Forests beat include, which were influenced by forest fires, Chakulia (1.86 km²), Mango (1.39 km²), Dalma (0.95 km²), Patmda (3.31 km²), Nutandih (1.03 km²), and Bhadodih (0.57 km²) (Table 3). The highest forest fire burnt area (3.31 km²) was located in the Patmda beat with 31 forest fire locations. Forest beat-wise analysis indicated that the maximum and minimum forest fire burnt area and number of forest fire locations were in six forest beats of DWS. During the field survey, forest fire locations were identified as smoke in Fig. 5. The maximum forest fire exhibited in the Mango beat, where a total forest fire burnt area in a 7-year period comprises 21.8 km² with 154 forest fire locations, followed by Patmda beat with 14.95 km² of forest fire locations 160. Forest beat of Chakulia, Dalma, Nutandih, and Bhadodih areas comprised with minimum forest fire burnt area of less than 10 km², and the number of forests fire locations area varies up to 125,

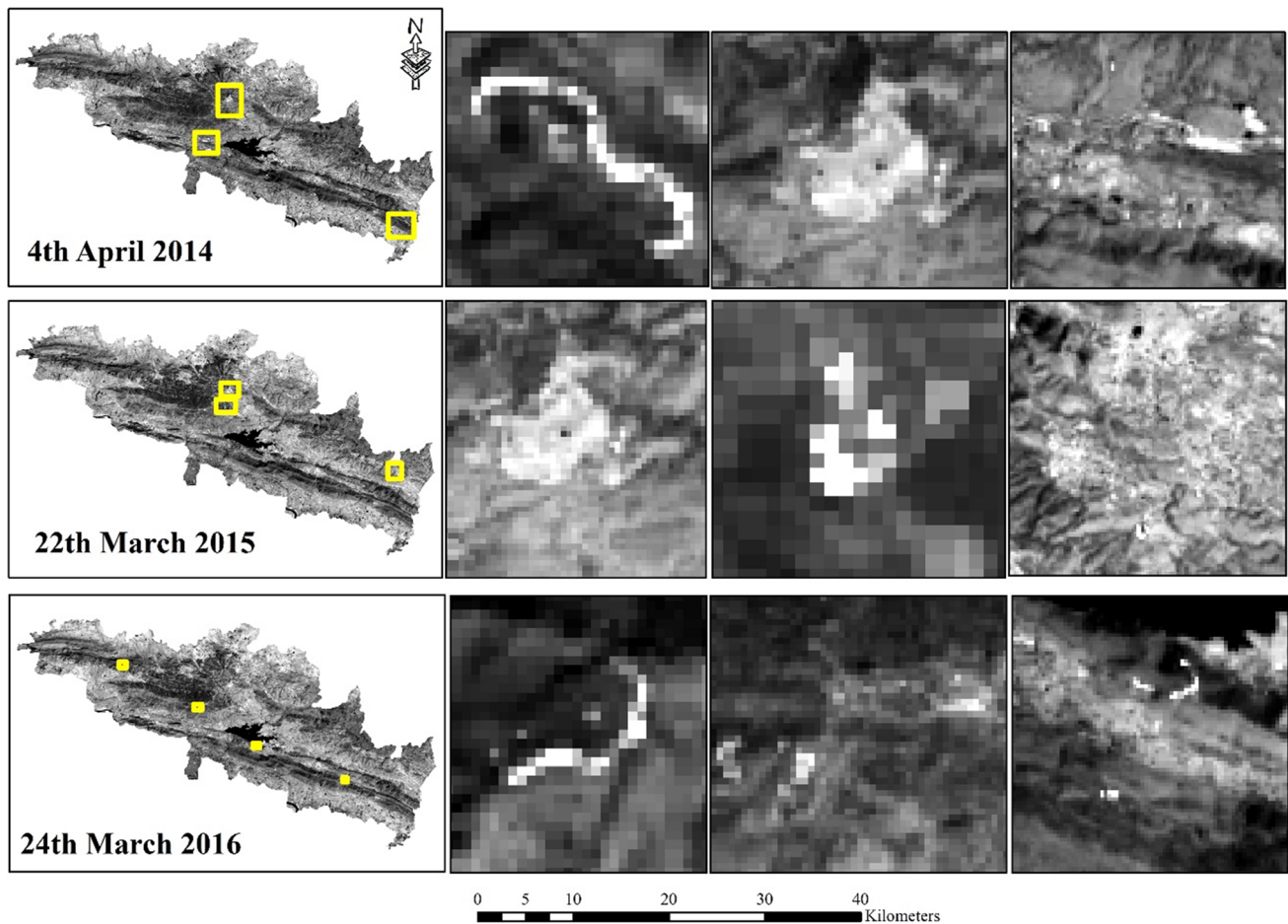


Fig. 7 Active forest fire pixel during the forest fire in different locations of DWS

Table 4 Beat-wise burned area (km²) as per the visual interpretation technique and the number of patches (shown in bracket)

| Beat | Area | Burnt area (patches) in 2014 | Burnt area (patches) in 2015 | Burnt area (patches) in 2016 | Burnt area (patches) in 2017 | Burnt area (patches) in 2018 | Burnt area (patches) in 2019 | Burnt area (patches) in 2020 |
|----------|-------|------------------------------|------------------------------|------------------------------|------------------------------|------------------------------|------------------------------|------------------------------|
| Chakulia | 62.71 | 0.42 km ² (17) | 0.519 km ² (34) | 2.25 km ² (48) | 1.86 km ² (26) | 0.45 km ² (13) | 0.38 km ² (19) | 0.1 km ² (1) |
| Mango | 79.61 | 4.06 km ² (21) | 10.40 km ² (61) | 5.95 km ² (49) | 1.39 km ² (23) | 8.43 km ² (52) | 2.91 km ² (28) | Nil (0) |
| Dalma | 61.95 | 1.69 km ² (18) | 1.20 km ² (22) | 5.67 km ² (29) | 0.95 km ² (23) | 1.34 km ² (19) | 1.05 km ² (21) | Nil (0) |
| Patmda | 58.75 | 2.44 km ² (29) | 6.19 km ² (64) | 3.01 km ² (36) | 3.31 km ² (31) | 5.1 km ² (42) | 2.6 km ² (24) | 0.4 km ² (2) |
| Nutandih | 53.63 | 1.78 km ² (20) | 3.12 km ² (35) | 2.29 km ² (70) | 1.03 km ² (16) | 2.7 km ² (36) | 1.8 km ² (27) | 0.3 km ² (2) |
| Bhadodih | 83.7 | 1.72 km ² (15) | 4.11 km ² (47) | 3.28 km ² (51) | 0.57 km ² (41) | 6.42 km ² (62) | 1.35 km ² (14) | 0.2 km ² (1) |
| Total | | 12.11 km ² | 25.5 km ² | 22.45 km ² | 9.11 km ² | 24.44 km ² | 10.09 km ² | 1.0 km ² |

92, 131, and 154. In this context, forest beat wise analysis for forest fire burnt area and number of forest fire locations was least in DWS as compared to fire density in terms of the number of forest fire and the pictorial graph 1, representing the forest fire burnt area statics.

In the year 2018, the total area influenced by forest fire was 28.73 km² and the total number of forest fire patches was observed to be 224. If we look at the beat-wise statistics

of forest fire, all six beats of DWS were influenced by forest fires, including Chakulia (0.45 km²), Mango (8.43 km²), Dalma (1.34 km²), Patamda (5.1 km²), Nutandih (2.7 km²), and Bhadodih (6.24 km²) (Table 4). The study exhibited that although maximum numbers of forest fire patches were found in Bhadudih, the area under maximum forest fire falls in Mango beat.

In the year 2019, the total area influenced by forest fire was 10.09 km², and the total number of forest fire patches was observed to be 133. Whereas, beat-wise observations include those influenced by forest fires at Chakulia (0.38 km²), Mango (2.91 km²), Dalma (1.05 km²), Patmda (2.6 km²), Nutandih (1.8 km²), and Bhadodih (1.35 km²) (Table 4). This present study has exhibited the maximum area influenced by forest fire was in the Mango beat, and the maximum number of forest fire patches was also seen in the Mango beat (Table 4).

In the year 2020, the total area affected by forest fire was 1 km², and the total number of forest fire patches was 6. It was observed that the fire occurrences were least in DWS in 2020 as compared to 2014 to 2019, which can be attributed to the COVID-19-induced pandemic and lockdown where most of the anthropogenic activities were minimal [50]. In 2020, the maximum affected area of forest fire was from the Patmda forest beat, where only two forest fire patches were observed (Table 4). Beat-wise

comparative results include Chakulia (0.1 km²), Mango (0.0 km²), Dalma (0.0 km²), Patmda (0.4 km²), Nutandih (0.3 km²), and Bhadodih (0.2 km²) (Table 4).

Forest burnt areas over 2014–2020 were overlaid over the forest density map in DWS (Fig. 8). It was observed that due to forest fires, the forest has been transferred mostly to the degraded forest, which comprises an area of 22.71 km² (11.13% of degraded forest) as of the year 2017. The maximum forest degradation was observed in the year 2016 due to the maximum number of forest fires observed. The forest has been transferred mostly from degraded forest to open forest, which comprises an area of 38.54 km² (18.89% of degraded forest) as per the year 2016.

4.4 Forest Fire Identification Based on NBR Index

The NBR index exhibits that the range for an active forest fire is from -0.6 to -0.07 , whilst the burnt area ranges from -0.07 to 0.02 in DWS from 2014 to 2020 (Fig. 6). The

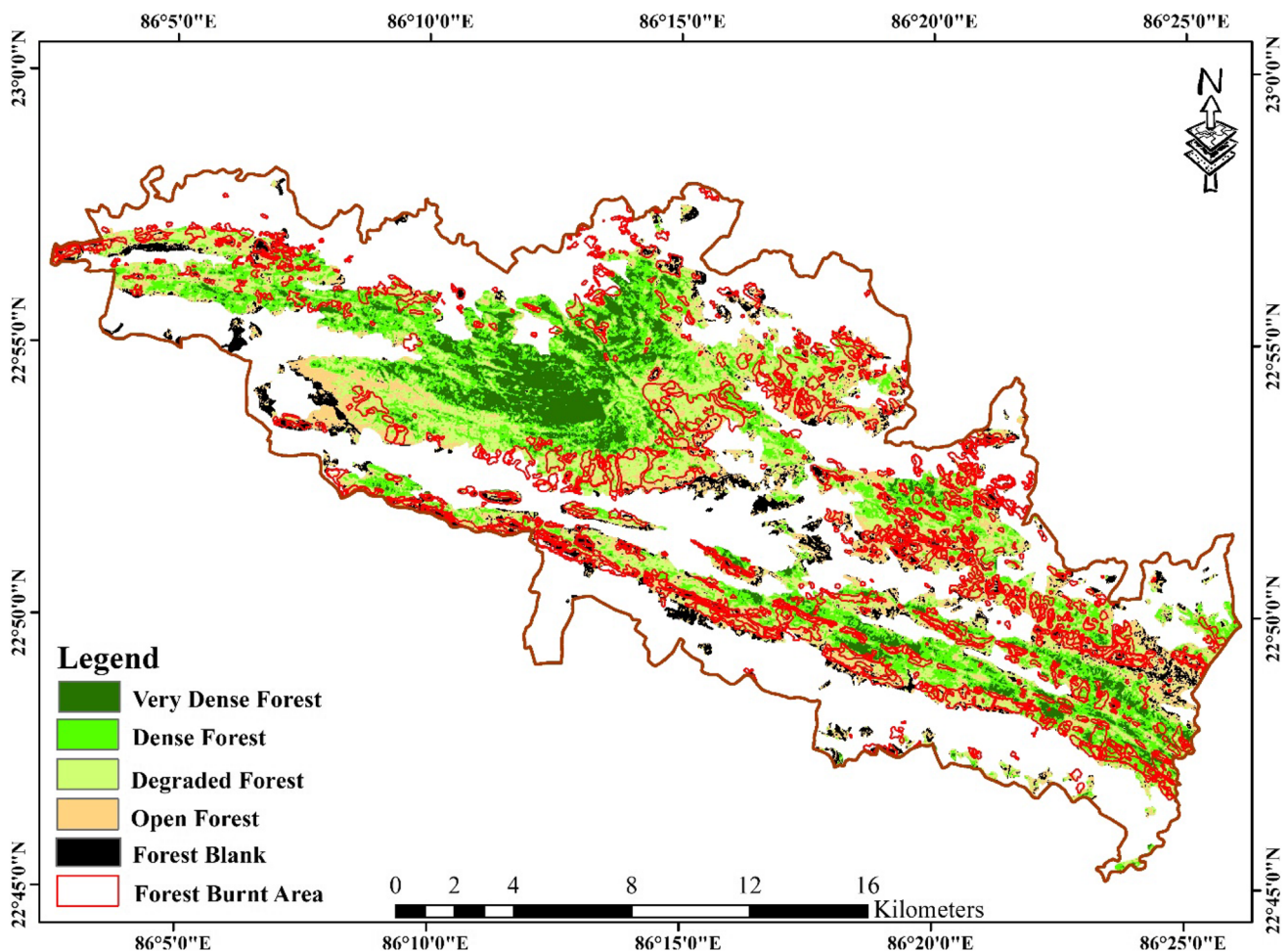


Fig. 8 Degraded forest overlaid by forest fire burnt area during the 2014 to 2020

maximum area under active burnt class was found in the year 2015 with an area of 1.24 km². The minimum active forest fire was found in the year 2020 with an area of only 0.05 km². In 2016, a total of 33.4 km² of the area was found to be burnt, which is the maximum for consecutive years. The least burnt area was found in the year 2020, with an area of only 1 km². The rest of the statistics found in the different years are mentioned in Fig. 9 and Table 5. Visual interpretation and NBR technique based on the forest fire burnt area analysis. It shows the most similar locations of forest fire, indicating in the forest burnt areas in both results.

4.5 Active Forest Fire Patches Inside NFB and Outside Notified Boundaries

In the present study, Forest fire and active forest fire patches locations were located each direction of the sanctuary. The major active forest fire locations are situated along with the road network and village of the sanctuary. Hence, forest patches that come under anthropogenic contact increase forest fires. In this context, it increases forest fire incidents within its time frame during the pre-monsoon season. It was

Table 5 Forest fire affected area (km²) during 2014 to 2020 in DWS using the NBR and visual interpretation (VI)

| Year's | NBR | FF burnt (VI) | Active fire |
|--------|-------|---------------|-------------|
| 2014 | 8.45 | 12.11 | 0.325 |
| 2015 | 25.74 | 25.5 | 0.232 |
| 2016 | 33.4 | 22.45 | 0.356 |
| 2017 | 9.91 | 9.11 | 0.066 |
| 2018 | 26.6 | 24.4 | 0.261 |
| 2019 | 11.4 | 10.09 | 0.18 |
| 2020 | 1.05 | 1.0 | 0.010 |

observed that forest fire-affected areas inside NFB as well as outside NFB (Fig. 10). The total area from active forest fires during 2014 to 2020 in the sanctuary was 1.43 km², and the total number of forest fires was 127. Whereas maximum forest fire inside the NFB was 1.01 km² and while outside NFB was 0.42 km². In addition, around 92 active forest fire areas were observed inside NFB, whereas 35 active forest fire area was outside NFB (Fig. 10).

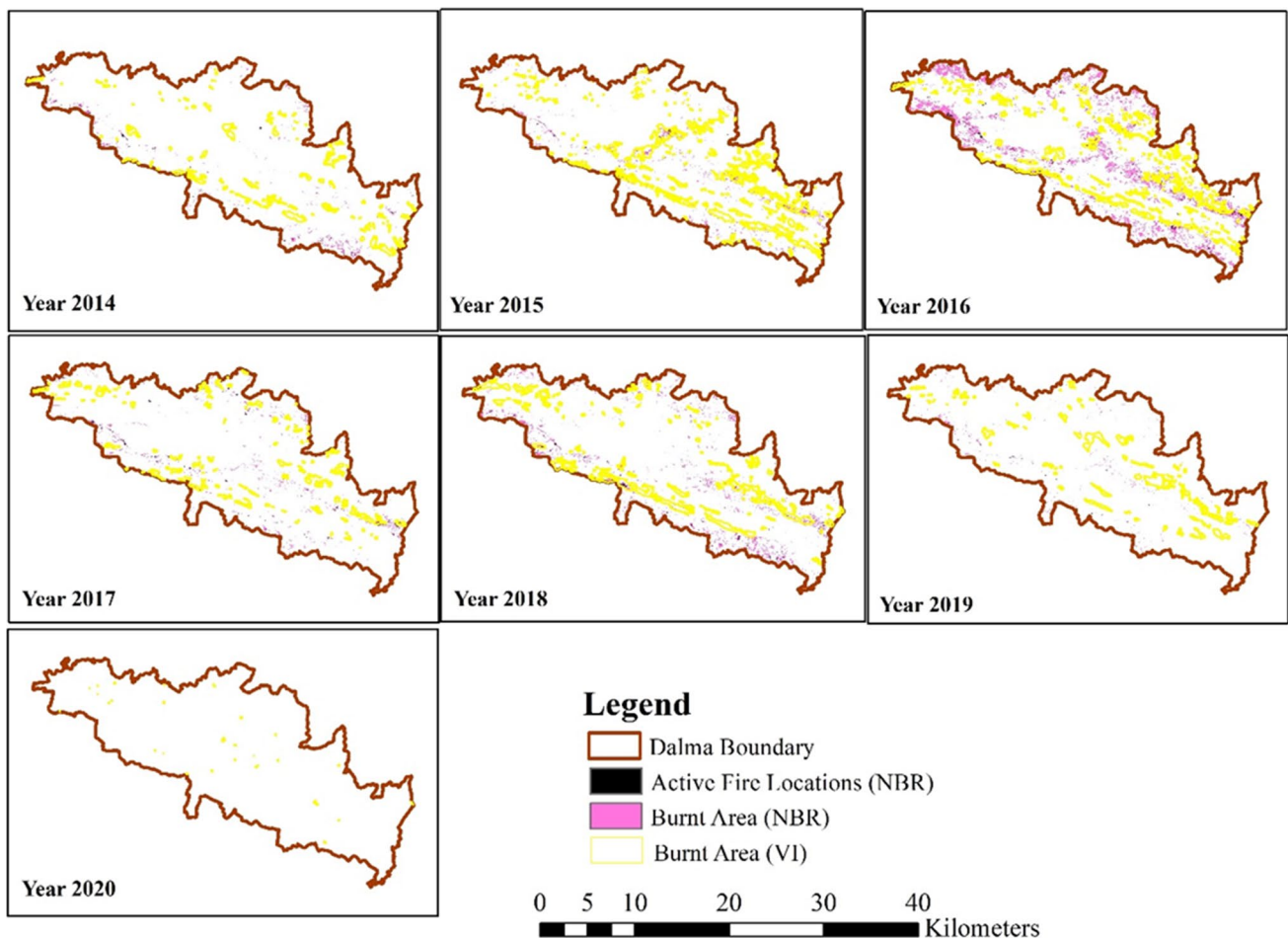


Fig. 9 Map showing active fire locations, burnt area using NBR, and visual interpretation based forest fire burnt area in DWS from 2014 to 2020

Fig. 10 Active forest fire patches during 2014–2020 inside NFB and outside NFB in DWS as prepared by visual analysis

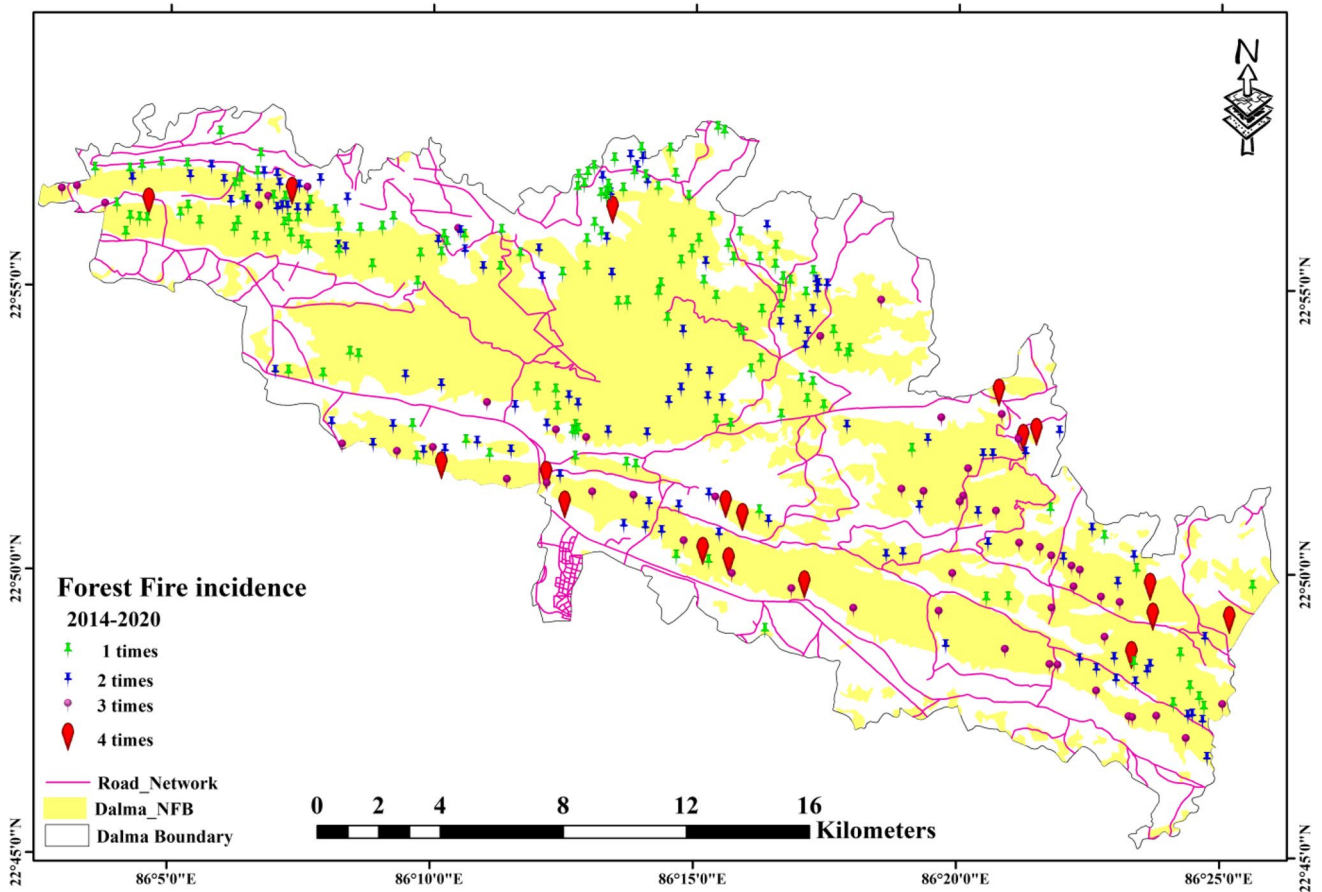
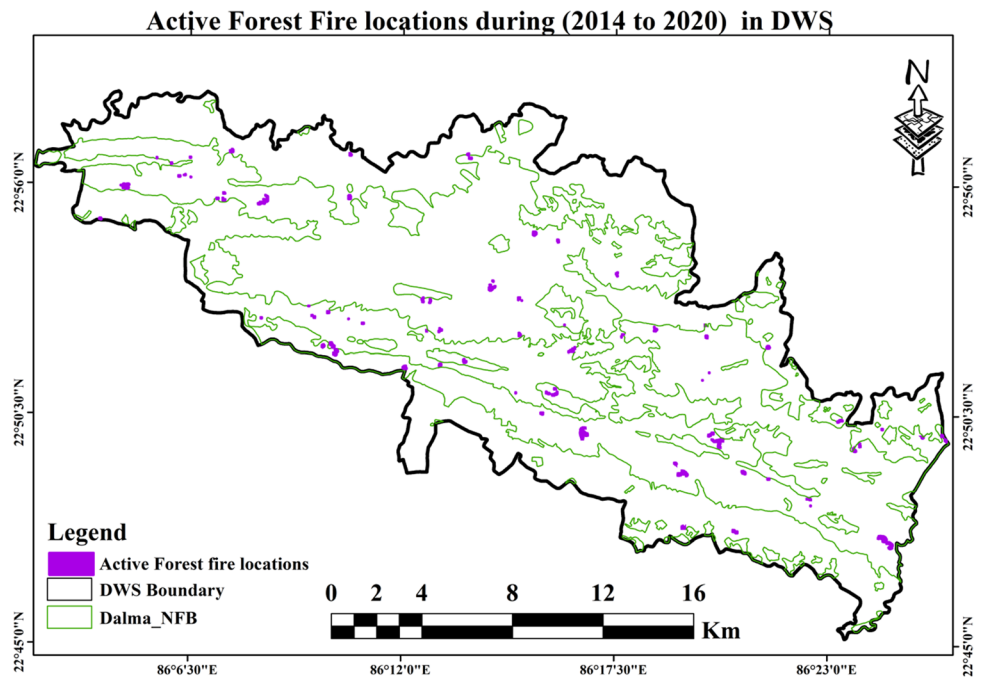


Fig. 11 Map representing recurrent forest fire locations during 2014–2020 in DWS

4.6 Forest Fire Recurrence Zone Mapping

The fire frequency map showed that the maximum occurrence of 3–4 times (high-risk zones) was observed mostly in proximity to roads during the 7 years over the span of 2014–2020 (Fig. 11). Among several beats, the Mango beat has displayed a fire frequency of 6 times. However, fire frequency of 1–2 times (low-risk zone) is distributed mostly over the interior or core regions of DWS. These results revealed that the major cause of recurrent forest fires in the sanctuary is primary the anthropogenic activity and expansion of road networks inside the sanctuary. Recurrent forest fires mainly focus on the area where forest fire incidents are actively performed from 2014 to 2020, as shown in Fig. 11.

An overall analysis of forest fire recurrence indicated that parts of the sanctuary are occupied by the human population, and major fire incidences occurred near the roads, built-up and agricultural land, mainly in the vicinity of degraded and open forests. The forest fire analysis in DWS indicates that the annual forest fire affected area lies in the dry deciduous

forests (degraded forest and open forest), which provide a major source of timber wood to local people.

5 Discussion

Forest fires constitute the most common hazard in forests and pose a threat not only to the forest wealth but also to the associated fauna and flora, disturbing the biodiversity, ecology, and environment of a region [51]. During the summer season, the forests become littered with dry senescent leaves and twinges, which could burst into flames ignited by the slightest spark [52]. In the present study, forest fire assessment in DWS was performed using Landsat-8 satellite data over the span of 2014 to 2020 for delineating forest fire-prone areas. The key findings indicate that forest fire was mostly identified in the degraded forest, open forest, and non-forest regions of DWS. The active fire season was seen from March to May, which is mostly ground fire rather than crown fire due to the presence of ground fuels or dry

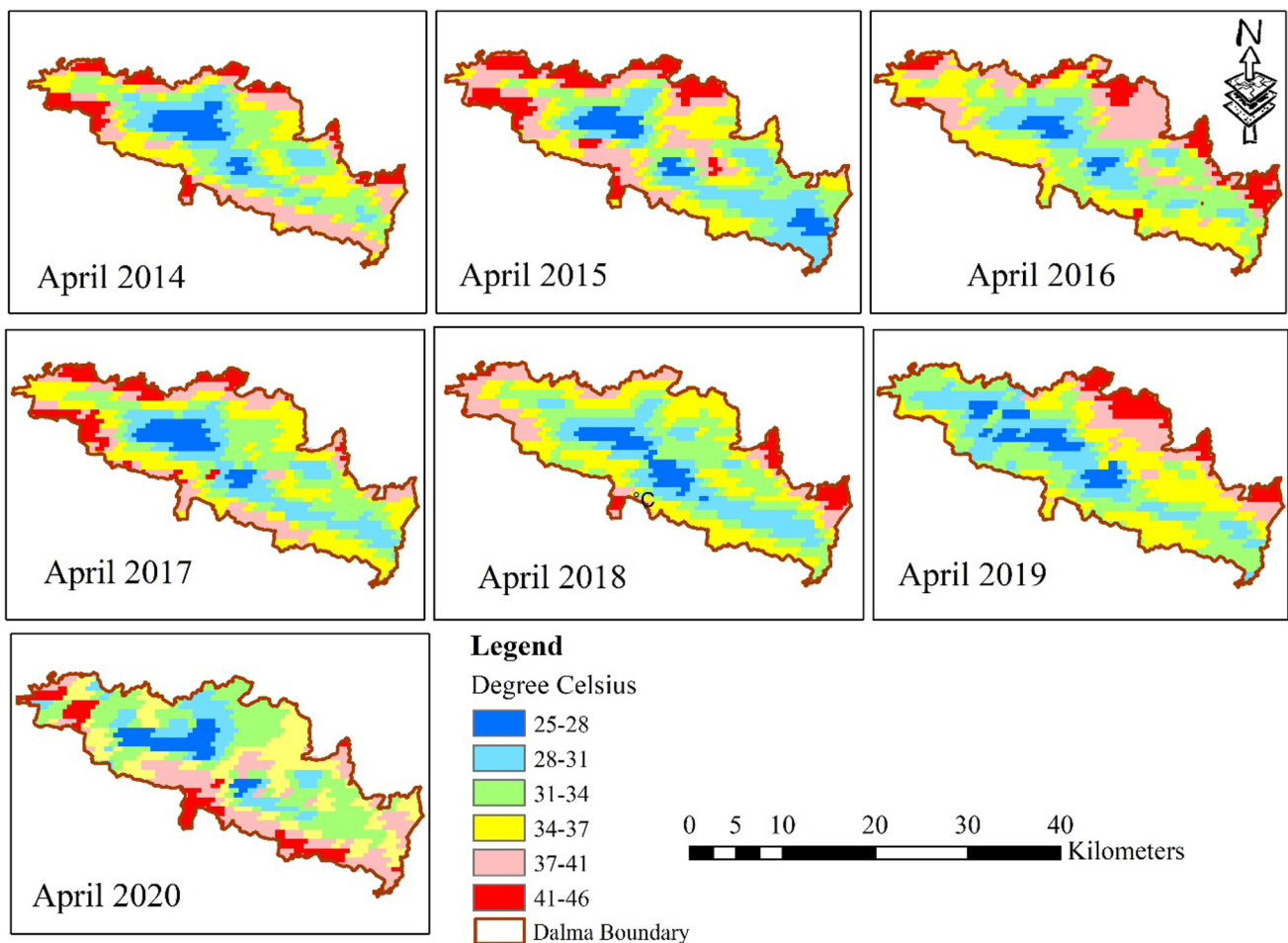


Fig. 12 Land surface temperature (LST) variation during forest fire from 2014 to 2020 in DWS

litter. Consequently, ground fire does not affect the crown of forests which is in line with other conclusions drawn from other areas in India [4]. In India, nearly 90% of fire ignitions are due to anthropogenic activities [10]. However, some latest studies on India indicated that maximum temperature is positively correlated with the burned area, including seasonal droughts and the global oscillation indices such as Niño-3.4) [4, 53]. Thereby, an increasing temperature over DWS due to global warming could potentially lead to severe forest fires in the future in combination with heat waves and long droughts. An analysis of land surface temperature (LST) indicated that temperature varies from 25 to 46 °C from April 2014 to 2020 in DWS (Fig. 12). The LST was higher persistently in the periphery regions of DWS, which is attributed to human activities (e.g., settlements, industry, construction, national highways, etc.), whereas it was lower in the core areas of forest. Among the last 7 years, the relatively higher LST was seen in the years 2015 and 2016, whereas the lowest LST was in 2020. The lower LST in 2020 is mostly attributed to the slow-down of anthropogenic activities due to COVID-19 [54]. The higher LST in April 2015, 2016, and 2018 also revealed a higher number of burn area patches (Table 4).

The forest beat wise analysis found that the Mango Forest beat has shown a maximum burned areas due to forest fires during 7 years of studies, and the main reason behind the occurrence of most forest fires was built-up land and national highways that passed through the sanctuary and nearby forest patches. A finding common to many of these studies is that the global thresholds used to narrow the search for fire pixels (the “potential fire thresholds”) are too high for some regions, rendering the algorithm unable to detect the (generally) smaller and/or cooler fires characteristic of these regions. Recently, the available VIIRS dataset provides fire pixel detection with a resolution of 375 × 375 m, making fire alerts more robust. This observation indicated all the incidents of forest fire happened over 7 years. Forest fire reoccurrence zone mapping indicates annual forest fire-affected area was found in degraded forest and open forest, which provides a major source of collections of fuel wood and other resources. The impact of forest fire damage in DWS involves not only the amount of timber burnt but also other natural resources, such as herbal plants, insects, and wildlife habitats.

6 Conclusion

Forest fires resulting in longer, hotter, and drier summers would increase the frequency of large forest fires and the length of fire seasons. This could lead to natural disturbance and ecological disasters in the forest ecosystem.

The present study revealed that forest fire is more dominant in Asanbani, Pardih, Bhelaipahari, Gobargushi, Bamri, Andharjhor, Somadih, Koira, Tetla, Bochkamkocha, Sah, Rbera, and Jamdih locations in DWS. The study also observed that the highest number of forest fires were recorded in the year 2015, with 29.61 km² of the area affected by forest fire, whereas the year 2020 observed the least forest fire burnt area showing to lockdown. Forest fire-affected area inside the NFB clearly indicates a lack of forest fire management practices. Most of the forest fires in DWS occurred in the degraded forest, where wild grasses and shrubs dominate, largely in the area where forest boundaries merge with agricultural lands, indicating possible anthropogenic influence in forest fire generation.

Encroachment in the forest land by removing the forest species for agricultural purposes and hunting during pre-monsoon (March–April) is a common phenomenon, leading to forest fires. An effective management plan for forest conservation and forest fire protection is required to protect forest resources in the DWS. The use of temporal remote sensing data and geospatial application is the most reliable and cost-effective approach for forest fire detection and monitoring. Nevertheless, increasing temperature, coupled with human intervention primarily during the summer season, could lead to an intense forest fire in the DWS.

Abbreviations DWS: Dalma Wildlife Sanctuary; TM: Thematic mapper; ETM + : Enhanced thematic mapper plus; OLI: Operational land imager; ISFR: Indian State of Forest Report

Acknowledgements The authors are thankful to the anonymous reviewers and editors for their valuable comments, which have brought vast changes to the present manuscript. The authors thank the Forest Department, Jharkhand, for providing the necessary information about the study area, i.e., Dalma Wildlife Sanctuary, Jharkhand, also USGS and Copernicus for making available Landsat and Sentinel data freely, which were used in the study.

Author Contribution The first author wrote the initial drafts of the manuscript with comments from the corresponding author. All authors together developed the ideas and framework for the manuscript. All authors read and approved the final version of the manuscript.

Data Availability All data generated or analyzed during this study are included in the manuscript.

Materials Availability All data generated or analyzed during this study are included in the manuscript.

Declarations

Ethics Approval and Consent to Participate Not applicable. This is original research.

Conflict of Interests The authors declare no competing interests.

References

- Moritz MA, Parisien M-A, Batllori E, Krawchuk MA, Van Dorn J, Ganz DJ, Hayhoe K (2012) Climate change and disruptions to global fire activity. *Ecosphere* 3:art49
- Mukhopadhyay A, Maulik U (2009) Unsupervised pixel classification in satellite imagery using multiobjective fuzzy clustering combined with SVM classifier. *IEEE Trans Geosci Remote Sensing* 47:1132–1138
- Whitlock C, Higuera PE, McWethy DB, Briles CE (2010) Paleoecological perspectives on fire ecology: revisiting the fire-regime concept. *TOECOLJ* 3:6–23
- Bar S, Parida BR, Roberts G, Pandey AC, Acharya P, Dash J (2021) Spatio-temporal characterization of landscape fire in relation to anthropogenic activity and climatic variability over the Western Himalaya, India. *GISci Remote Sens* 58:281–299
- Parida BR, Pandey AC, Patel NR (2020) Greening and browning trends of vegetation in India and their responses to climatic and non-climatic drivers. *Climate* 8:92
- Schoennagel T, Veblen TT, Romme WH (2004) The interaction of fire, fuels, and climate across rocky mountain forests. *Bioscience* 54:661
- Gharun M, Turnbull TL, Adams MA (2013) Stand water use status in relation to fire in a mixed species eucalypt forest. *For Ecol Manage* 304:162–170
- Chaudhary SK, Pandey AC, Parida BR, Gupta SK (2022) Using geoinformatics to link forest fire severity and fragmentation in India's Dalma Wildlife Sanctuary. *Trop Ecol* 63:53–462
- Jaiswal RK, Mukherjee S, Raju KD, Saxena R (2002) Forest fire risk zone mapping from satellite imagery and GIS. *Int J Appl Earth Obs Geoinf* 4:1–10
- Dobriyal M, Bijalwan A (2017) Forest fire in western Himalayas of India: a review. *N Y Sci J* 10:39–46
- Bar S, Parida BR, Pandey AC (2020) Landsat-8 and Sentinel-2 based forest fire burn area mapping using machine learning algorithms on GEE cloud platform over Uttarakhand, Western Himalaya. *Remote Sens Appl: Soc Environ* 18:100324
- Kunwar RM, Khaling S (2006) Forest fire in the Terai, Nepal: causes and community management interventions. *Int For Fire News* 34:46–54
- Krivtsov V, Vigy O, Legg C, Curt T, Rigolot E, Lecomte I, Jap-piot M, Lampin-Maillet C, Fernandes P, Pezzatti GB (2009) Fuel modelling in terrestrial ecosystems: an overview in the context of the development of an object-orientated database for wild fire analysis. *Ecol Model* 220:2915–2926
- Vadrevu KP, Giglio L, Justice C (2013) Satellite based analysis of fire-carbon monoxide relationships from forest and agricultural residue burning (2003–2011). *Atmos Environ* 64:179–191
- Roy DP, Jin Y, Lewis PE, Justice CO (2005) Prototyping a global algorithm for systematic fire-affected area mapping using MODIS time series data. *Remote Sens Environ* 97:137–162
- Sudhakar Reddy C, Vazeed Pasha S, Jha CS, Dadhwal VK (2015) Geospatial characterization of deforestation, fragmentation and forest fires in Telangana state, India: conservation perspective. *Environ Monit Assess* 187:455
- Ahmad S, Pandey AC, Kumar A, Parida BR, Lele NV, Bhattacharya BK (2020) Chlorophyll deficiency (chlorosis) detection based on spectral shift and yellowness index using hyperspectral AVIRIS-NG data in Sholayar reserve forest, Kerala. *Remote Sens Appl: Soc Environ* 19:100369
- Zhiliang Zhu, Carl Key, Donald Ohlen, Nate Benson (2006) Evaluate sensitivities of burn-severity mapping algorithms for different ecosystems and fire histories in the United States. <https://doi.org/10.5962/bhl.title.154495>
- Chuvieco E (2009) Earth observation of wildland fires in Mediterranean ecosystems. Springer
- Szpakowski D, Jensen J (2019) A review of the applications of remote sensing in fire ecology. *Remote Sens* 11:2638
- Chen T-H, Wu P-H, Chiou Y-C (2004) An early fire-detection method based on image processing. In: 2004 International Conference on Image Processing, 2004. ICIP'04. IEEE, pp 1707–1710
- Fang L, Yang J, Zu J, Li G, Zhang J (2015) Quantifying influences and relative importance of fire weather, topography, and vegetation on fire size and fire severity in a Chinese boreal forest landscape. *For Ecol Manage* 356:2–12
- Quintano C, Fernández-Manso A, Fernández-Manso O (2018) Combination of Landsat and Sentinel-2 MSI data for initial assessing of burn severity. *Int J Appl Earth Obs Geoinf* 64:221–225
- Clark J, Parsons A, Zajkowski T, Lannom K (2003) Remote sensing imagery support for burned area emergency response teams on 2003 southern California wildfires. USFS Remote Sens Appl Center BAER Support Summary
- Fernandez-Manso A, Quintano C, Roberts DA (2016) Burn severity influence on post-fire vegetation cover resilience from Landsat MESMA fraction images time series in Mediterranean forest ecosystems. *Remote Sens Environ* 184:112–123
- Navarro G, Caballero I, Silva G, Parra P-C, Vázquez Á, Caldeira R (2017) Evaluation of forest fire on Madeira Island using Sentinel-2A MSI imagery. *Int J Appl Earth Obs Geoinf* 58:97–106
- van der Werf GR, Randerson JT, Giglio L, Gobron N, Dolman AJ (2008) Climate controls on the variability of fires in the tropics and subtropics: climate controls on fires. *Glob Biogeochem Cycles* 22:GB3028
- Shoko C, Mutanga O (2017) Seasonal discrimination of C3 and C4 grasses functional types: an evaluation of the prospects of varying spectral configurations of new generation sensors. *Int J Appl Earth Obs Geoinf* 62:47–55
- van Wagtenonk JW, Root RR, Key CH (2004) Comparison of AVIRIS and Landsat ETM+ detection capabilities for burn severity. *Remote Sens Environ* 92:397–408
- Smith AMS, Wooster MJ, Drake NA, Dipotso FM, Falkowski MJ, Hudak AT (2005) Testing the potential of multi-spectral remote sensing for retrospectively estimating fire severity in African Savannas. *Remote Sens Environ* 97:92–115
- Robichaud PR, Lewis SA, Laes DYM, Hudak AT, Kokaly RF, Zamudio JA (2007) Postfire soil burn severity mapping with hyperspectral image unmixing. *Remote Sens Environ* 108:467–480
- Lewis SA, Lentile LB, Hudak AT, Robichaud PR, Morgan P, Bobbitt MJ (2007) Mapping ground cover using hyperspectral remote sensing after the 2003 Simi and Old wildfires in Southern California. *Fire Ecol* 3:109–128
- Robinson NM, Leonard SWJ, Bennett AF, Clarke MF (2014) Refuges for birds in fire-prone landscapes: the influence of fire severity and fire history on the distribution of forest birds. *For Ecol Manage* 318:110–121
- Giglio L, Boschetti L, Roy DP, Humber ML, Justice CO (2018) The collection 6 MODIS burned area mapping algorithm and product. *Remote Sens Environ* 217:72–85
- Csiszar I, Schroeder W, Giglio L, Ellicott E, Vadrevu KP, Justice CO, Wind B (2014) Active fires from the Suomi NPP visible infrared imaging radiometer suite: product status and first evaluation results. *J Geophys Res: Atmos* 119:803–816
- Freeborn PH, Wooster MJ, Roy DP, Cochrane MA (2014) Quantification of MODIS fire radiative power (FRP) measurement uncertainty for use in satellite-based active fire characterization and biomass burning estimation. *Geophys Res Lett* 41:1988–1994
- Hantson S, Arneeth A, Harrison SP, Kelley DI, Prentice IC, Rabin SS, Archibald S, Mouillot F, Arnold SR, Artaxo P (2016) The

- status and challenge of global fire modelling. *Biogeosciences* 13:3359–3375
38. Wang X, He HS, Li X (2007) The long-term effects of fire suppression and reforestation on a forest landscape in Northeastern China after a catastrophic wildfire. *Landsc Urban Plan* 79:84–95
 39. Ressler R, Lopez G, Cruz I, Colditz RR, Schmidt M, Ressler S, Jiménez R (2009) Operational active fire mapping and burnt area identification applicable to Mexican Nature Protection Areas using MODIS and NOAA-AVHRR direct readout data. *Remote Sens Environ* 113:1113–1126
 40. Cheng D, Rogan J, Schneider L, Cochrane M (2012) Evaluating MODIS active fire products in subtropical Yucatán forest. *Remote Sens. Lett* 4:455–464
 41. Kumari B, Pandey AC (2020) MODIS based forest fire hotspot analysis and its relationship with climatic variables. *Spat Inf Res* 28:87–99
 42. ISFR (2019) India state of forest report. Forest Survey of India, Ministry of Environment, Forest and Climate Change (MoEFCC), Dehradun
 43. Chatterjee ND (2016) Man-elephant conflict: a case study from forests in West Bengal. Springer, India
 44. Dennison PE, Brewer SC, Arnold JD, Moritz MA (2014) Large wildfire trends in the western United States, 1984–2011. *Geophys Res Lett* 41:2928–2933
 45. Keeley JE (2009) Fire intensity, fire severity and burn severity: a brief review and suggested usage. *Int J Wildland Fire* 18:116–126
 46. Schroeder W, Oliva P, Giglio L, Quayle B, Lorenz E, Morelli F (2016) Active fire detection using Landsat-8/OLI data. *Remote Sens Environ* 185:210–220
 47. King MD, Platnick S, Moeller CC, Revercomb HE, Chu DA (2003) Remote sensing of smoke, land, and clouds from the NASA ER-2 during SAFARI 2000. *J Geophys Res: Atmos* 108:8502
 48. Cadau E, Laneve G (2008) Improved MSG-SEVIRI images cloud masking and evaluation of its impact on the fire detection methods. In: IGARSS 2008–2008 IEEE Int Geosci Remote Sens Symp. IEEE, p II–1056
 49. Ho Y, Wookey S (2019) The real-world-weight cross-entropy loss function: modeling the costs of mislabeling. *IEEE Access* 8:4806–4813
 50. Parida BR, Bar S, Singh N, Oinam B, Pandey AC, Kumar M (2021) A short-term decline in anthropogenic emission of CO₂ in India due to COVID-19 confinement. *Prog Phys Geogr: Earth Environ* 45:471–487
 51. Parashar A, Biswas S. The impact of forest fire on forest biodiversity in the Indian Himalayas (Uttaranchal). In: XII World Forestry Congress, vol 358
 52. Srivastava S, Dvivedi A, Shukla RP (2014) Invasive alien species of terrestrial vegetation of north-eastern Uttar Pradesh. *Int J For Res* 2014:1–9
 53. Pausas JG, Ribeiro E (2013) The global fire-productivity relationship: fire and productivity. *Glob Ecol Biogeogr* 22:728–736
 54. Parida BR, Bar S, Roberts G, Mandal SP, Pandey AC, Kumar M, Dash J (2021) Improvement in air quality and its impact on land surface temperature in major urban areas across India during the first lockdown of the pandemic. *Environ Res* 199:111280

Publisher's Note Springer Nature remains neutral with regard to jurisdictional claims in published maps and institutional affiliations.

Springer Nature or its licensor holds exclusive rights to this article under a publishing agreement with the author(s) or other rightsholder(s); author self-archiving of the accepted manuscript version of this article is solely governed by the terms of such publishing agreement and applicable law.